09

Solid state quantum memory for optical signal at the single-photon level

© R.A. Akhmedzhanov, L.A. Gushchin, I.V. Zelensky, V.A. Nizov, N.A. Nizov, D.A. Sobgaida

Federal Research Center A.V. Gaponov-Grekhov Institute of Applied Physics of the Russian Academy of Sciences,
603950 Nizhny Novgorod, Russia
e-mail: zelensky@ipfran.ru

Received April 21, 2025
Revised April 21, 2025
Accepted April 21, 2025

We implement solid state quantum memory for optical signal at the single-photon level based on atomic frequency comb protocol in an isotopically pure $^{143}Nd^{3+}:Y^7LiF_4$ crystal. Using weakened laser pulses with the average photon number of around 1 we demonstrate signal storage for 60 ns with an efficiency of 6.4 % and a signal-to-noise ratio ~ 3. We create single-photon source based on spontaneous parametric down-conversion spectrally matched with quantum memory, and demonstrate the storage of its signal.

Keywords: atomic frequency comb, spontaneous parametric down-conversion, heralded single-photon source.

DOI: 10.61011/TP.2025.10.62074.65-25

Introduction

Advancement in quantum technologies has promoted extensive research efforts for creating quantum memory capable of handling optical signals at the single-photon level [1]. Implementation of compact and easy-to-use solid-state devices is of special interest. Rare-earth-ion-doped crystals are currently considered as the most promising basic components for such devices [2–5]. In such systems, 4f electron shells are partially shielded from the crystalline environment by full outer shells [6]. This leads to long population and coherence lifetimes that are necessary for effective long-term memory.

To date, several approaches to implementing quantum memory with rare-earth ions have been demonstrated [7–12]. The authors of this work have used the atomic frequency comb (AFC) protocol [13] offering a set of advantages: high multimode capacity [14,15], simplicity of experimental implementation and relatively high efficiency. The essence of the protocol is as follows. A periodic absorption profile is burned out by laser light in an inhomogeneously broadened transition. When an optical pulse with a spectrum corresponding to the structure width enters this medium, it is absorbed (written) and then reemitted (read) after a time inversely proportional to the comb period.

To create a quantum memory, this study used an isotopically pure $^{143}Nd^{3+}:Y^7LiF_4$ crystal cooled to cryogenic temperatures. Neodymium ions in this crystal have a strong optical transition with a wavelength about 867 nm lying within an optical fiber transmission window. Transitions in isotopically pure crystals have small inhomogeneous broadening (~ 100 MHz in our case), which makes it possible to select the desired working line within the complicated transition structure. Moreover, such crystals usually demonstrate a lower decoherence rate. We have previously investigated AFC-based optical memory in this crystal using „bright" multiphoton pulses [16–18]. This work addresses memory implementation at the single-photon level.

Laser pulses weakened to the single-photon level were used in the first part. Necessary parameters were chosen and a quantum memory was created to handle such weak signal. Note that storage of nonclassical states from single photon sources is critical for many technologies, in particular, for creating extended quantum communications using quantum repeaters [19]. The second part of the study describes the usage of the created memory for solving of this problem. For this, an appropriate source was required.

Spontaneous parametric down conversion (SPDC) [20] in a periodically-poled lithium niobate crystal doped with magnesium oxide, MgO:PPLN, was used to generate single photons. Advantage of SPDC is in the fact that photons are produced in pairs during the down-conversion. Detection of one of them heralds the creation of the photon pair. Periodically-poled crystals provide a collinear generation mode allowing for temperature wavelength tuning [21]. This tuning mechanism is convenient for matching the memory frequency. However, a typical width of such source (with a crystal length of 20–30 mm) is ~ 100 GHz [22], which is approximately 1000 times larger than the spectral bandwidth of our memory. To solve this problem, a spectrally matched filtration system was implemented for both source channels using the Fabry–Perot interferometers.

1. Quantum memory with weakened laser pulses

A quantum memory implementation setup is shown in Figure 1. An isotopically pure $^{143}Nd^{3+}:Y^7LiF_4$ crystal (content of ^{7}Li isotope ~ 99.7 %) with neodymium ion content of 0.005 at.% (content of $^{143}Nd^{3+}$ ~ 96.5 %), 5 mm in length, cut along the c axis was used as the active

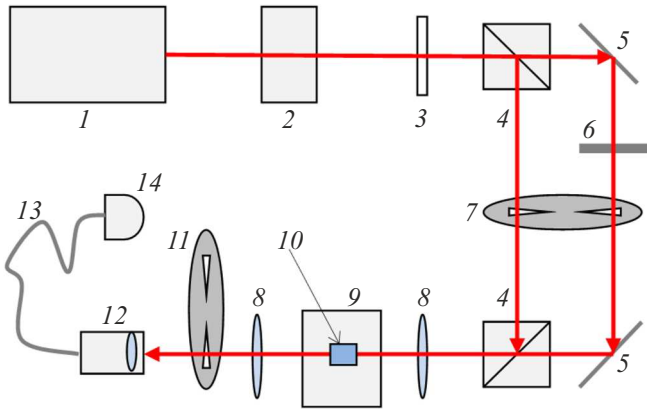

Figure 1. Schematic diagram of a quantum memory system with weakened laser pulses: *1* — laser, *2* — AOM, *3* — half-wave plate, *4* — polarizing beam splitter, *5* — mirrors, *6* — light filters, *7, 11* — optical choppers, *8* — lenses, *9* — cryostat, *10* — $^{143}Nd^{3+}:Y^7LiF_4$ crystal, *12* — collimator, *13* — optical fiber, *14* — single-photon detector.

medium. The crystal was placed into an optical cryostat and cooled to ~ 4 K.

AFC was created at the $^4I_{9/2}(1)-^4F_{3/2}(1)$ transition (~ 867 nm) using single-frequency titanium-sapphire laser radiation. Laser frequency was stabilized by a wavelength meter providing a long-term drift of max. 5 MHz. Laser light could be frequency-/intensity-modulated using an acousto-optic modulator (AOM). Various approaches may be used to create the AFC [18]. In one such approach, the comb is burned in the inhomogeneously broadened line using relatively long pulses, the frequencies of which are varied stepwise (these frequencies correspond to the AFC absorption minima). This allows us to transfer a part of absorbing ions to other levels, leaving only the profile corresponding to the comb. Another approach uses short monochromatic pulses repeated at equal time intervals. The spectrum of such pulse sequence is a set of equidistant peaks, and the AFC period is determined by the time between pulses. Both approaches have their advantages and disadvantages, in particular, in the first approach it is possible to change the comb shape to optimize the memory efficiency. The second approach has a fixed AFC shape. However, this approach is free of beam walk during frequency tuning (done using the acousto-optic modulator). This simplifies spatial alignment of the AFC burning and written radiation. Both approaches were used. The first approach gave the best results in the experiments with weakened laser pulses, and the second approach was more convenient for handling the single-photon source.

For quantum memory operation, the memory cell shall be effectively matched with written signal. Since employment of fixed-polarization radiation was implied in our case, then a polarizing beam splitter was proposed for this purpose. Such approach can be used to combine the radiation from two different sources almost without loss. The important feature of the configuration is the fact that AFC is created using one polarization of the optical radiation, while the orthogonal polarization is used for the pulse to be written.

Experiments with „bright“ pulses were conducted to verify the proposed approach. Laser light was divided into two orthogonally polarized beams using the polarizing beam splitter. The beams were modulated by a rotating chopper in such a way that one beam was open in the first half-period and the other beam was open in the second half-period. Then, the beams were aligned on the second polarizing beam splitter. The experiments have proved that the proposed configuration was fully functional. Quantum memory efficiency for the case with different polarizations of the burnout and written radiations was a little lower than in the case of the same polarization and depended primarily on the degree of beam alignment.

The same configuration was used for experiments with weakened radiation. In this case, optical filters were placed in the signal channel. A superconducting nanowire single-photon detector (SNSPD) was used to detect weak pulses. SNSPD provided an efficiency of $\sim 85\%-90\%$ with intrinsic noise of about 25 cps. During the time when memory wasn't used, the detector was blocked by the second chopper that rotated synchronously with the first one.

AFC-based optical memory can theoretically handle a signal with intensity as low as desired. For practical implementation, noise is the only limitation for handling a weak signal. In our case, the fluorescence signal of neodymium ions excited to the upper level during comb preparation is the main source of noise. Introduction of a delay between the memory preparation and utilization is the most accessible residual fluorescence control method [23]. Note that AFC degrades with time, leading to a reduction in efficiency. Thus, the optimum delay will be determined as a trade-off between these processes.

Dependence of the fluorescence signal on time after AFC creation was measured. Since the fluorescence intensity weakly depends on direction, observations were carried out at an angle to the system axis. Thus, direct and scattered laser light was avoided, which was checked by the absence of signal when the laser wavelength was tuned away from the transition.

The measurements are shown in Figure 2. Fluorescence intensity decays exponentially. The decay law is adequately approximated by $F = Ae^{-t/\tau} + N$, with $\tau \approx 613\,\mu$s and $N \approx 25$ cps. Time τ corresponds to typical population lifetimes at the upper level [24]. Dark count N is corresponds to the intrinsic noise of SNSPD. During the time of 5 ms, fluorescence intensity decays to ~ 65 cps.

Dependence of the quantum memory efficiency on time after AFC creation measured using „bright“ pulses is shown in Figure 3. Due to the linearity of the AFC-based memory, efficiency is independent of intensity, therefore the measured dependence may be considered to be a good estimate

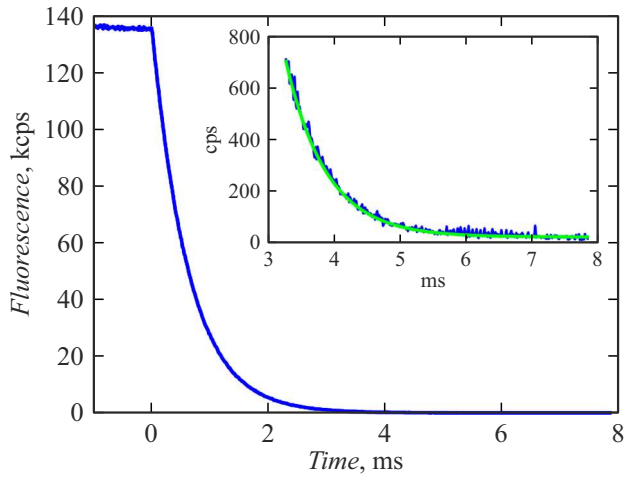

Figure 2. Fluorescence decay after AFC creation, the inset shows a magnified „tail“ of the dependence and exponential approximation.

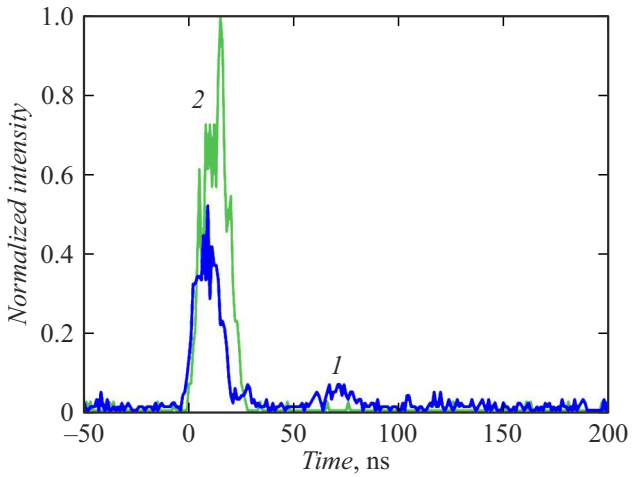

Figure 4. *1* — echo from the weakened laser light, *2* — incoming pulse.

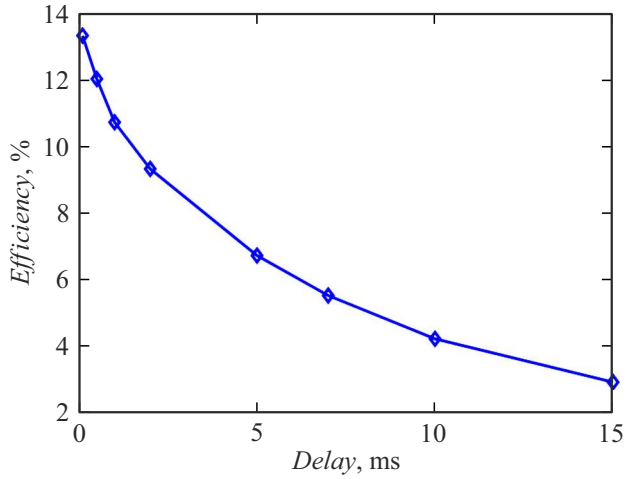

Figure 3. Quantum memory efficiency depending on time after AFC creation.

for weak signals. The figure shows that efficiency decays approximately by half during 5 ms and longer delays are not reasonable. Thus, 5 ms may be taken as the best delay time between AFC creation and utilization.

Experiment for memory implementation at a single-photon level was performed as follows. Chopper *7* (Figure 1) worked at 33 Hz. AFC was prepared in the first half-period. For this a sequence of 6 pulses with a power of about 30 mW and duration of 50 μs at different frequencies with 16 MHz steps was used. The procedure was repeated 40 times, with the total burning sequence time being 12 ms. After this, the burning beam was blocked and the written beam was opened. Simultaneously, the detector blocked by the chopper 11 during the memory creation sequence was also opened. In 5 ms after AFC creation, pulses with a duration of 20 ns weakened by optical filters to the energy corresponding to a average number of photons per pulse of ~ 1 were written into the memory. Since the intensity of such pulses is too low to damage the comb, a series of 100 pulses separated by an 10 μs interval was used. This made it possible to reduce the integration time that was necessary to obtain statistically relevant results. To determine the memory efficiency, response from the incoming pulse was measured at the same parameters, but at a wavelength lying outside the signal transition.

The results are presented in Fig. 4. An echo can be seen after the written pulse, after a period of 60 ns corresponding to the inverse AFC period. Memory efficiency defined as an echo and incoming pulse intensity ratio was equal to 6.4 %. This is similar to the memory efficiency obtained with the classical „bright“ signal. Signal-to-noise ratio under the measurement conditions is ~ 3.

2. Single-photon source signal storage

In terms of possible utilization, it was necessary to check whether the implemented quantum memory could be used to store a signal from the separate single-photon sources. For this, an SPDC-based single-photon source spectrally matched with the AFC was created.

Schematic diagram of the source is shown in Figure 5. Linearly polarized 532 nm pumping laser light was focused into the MgO:PPLN crystal with a period of 7.237 μm and length of 30 mm placed into the thermostat. Focal distance of the lens was equal to 150 mm, so that, with a pumping beam diameter of ~ 1 mm, a waist diameter of ~ 100 μm and Rayleigh length of ~ 30 mm similar to the crystal length were obtained. For adjustment of the polarization required for effective parametric down-conversion, a half-wave plate mounted in a rotating frame was used. A pump photon in the MgO:PPLN crystal split into a signal photon and heralding photon, whose frequencies were related as

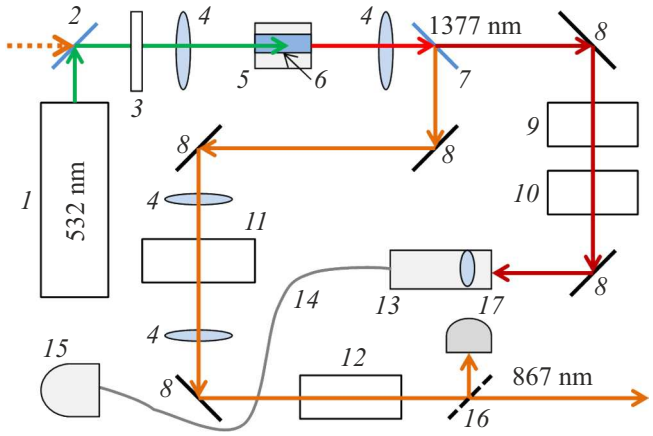

Figure 5. Single-photon source: *1* — 532 nm laser, *2* — dichroic mirror, *3* — half-wave plate, *4* — lenses, *5* — thermostat, *6* — MgO : PPLN crystal, *7* — dichroic mirror, *8* — totally reflecting mirrors, *9–12* — Fabry–Perot etalons, *13* — collimator, *14* — optical fiber *15* — single-photon detector, *16* — tilting mirror, *17* — photodiode. Dashed line shows radiation input for source tuning.

follows:

$$\nu_p = \nu_s + \nu_i, \tag{1}$$

where ν_p, ν_s, ν_i are pump, signal and heralding photon frequencies, respectively.

Signal radiation wavelength of 867 nm corresponded to heralding radiation wavelength of 1377 nm. They were separated using a dichroic mirror. The heralding photon passed through the filtration system and entered the superconducting detector, and its detection signaled a photon present in the signal channel. Generation wavelength in a periodically poled crystal depends linearly on temperature. The dependence parameters were measured using a technique identical to that described in [22]. Source radiation reflected from the diffraction grating was collimated into a single-mode fiber and then detected by SNSPD. Different grating positions corresponded to the maximum signal at different temperatures. Titanium sapphire laser, whose wavelength was measured by the wavelength meter, was used to calibrate that „monochromator“. Temperature dependence of the signal channel was 0.44 nm per degree. Quantum memory wavelength corresponds to 46.1 °C.

The maximum spectral width of quantum memory is limited by inhomogeneous broadening of the utilized transition and is equal to ~ 100 MHz. A spectral filtration system was implemented to narrow the source spectrum down to the desired value. The signal channel included the following components: a thermally-stabilized Fabry–Perot etalon *12* (Figure 5) with a free spectral range (FSR) of 20 GHz, peak width of about 1.5 GHz, and a transmission coefficient 80 % and a confocal Fabry–Perot interferometer *11* with a peak width of about 100 MHz.

Filters could be tuned within the FSR using the temperature and voltage at the piezoelements. Thermostabilization provided frequency stability within FWHM of the line at times of about 1 h for the etalon and ~ 15 min for the interferometer.

To control the quality of filter setting to the quantum memory frequency and periodic adjustment, AFC-producing laser radiation was used, for which it was brought into the source through a dichroic mirror and aligned with the pumping laser radiation. The signal was detected using a photodiode.

Confocal interferometer was the most difficult filtration system component to tune. It can work in two modes. In normal mode, it has FSR of 3 GHz and a transmission coefficient of 40 %–45 %. With accurate spatial matching of input radiation with the fundamental mode of the cavity, odd mode suppression mode is implemented. In this case, the interferometer has doubled FSR of 6 GHz and a transmission coefficient of 80 %–90 %. The second mode is preferable both in terms of the effective signal transmission and the spurious signal suppression. Unfortunately, fine tuning is required for this mode and can be accomplished only using supplementary laser light. The following interferometer tuning technique was proposed. When there are no filters in the heralding channel, the correlation function between the channels has a spiked form. Even and odd peaks generally may have different heights. Correlation function, where uniform drop of peak amplitude is observed, corresponds to the mode with FSR of 6 GHz (Figure 6).

Signal channel filtration leads to heralding efficiency reduction (ratio of the number of pairs to the number of heralding photons). This may be avoided, if only spectrally-conjugate heralding photons, i.e. those satisfying condition (1), are detected. The filtration system was based on the following assumptions: typical stability time was ~ 1 h, and drift of all parameters during the specified time should not lead to channel mismatch. Pump laser used in the source had a frequency drift of about 300 MHz

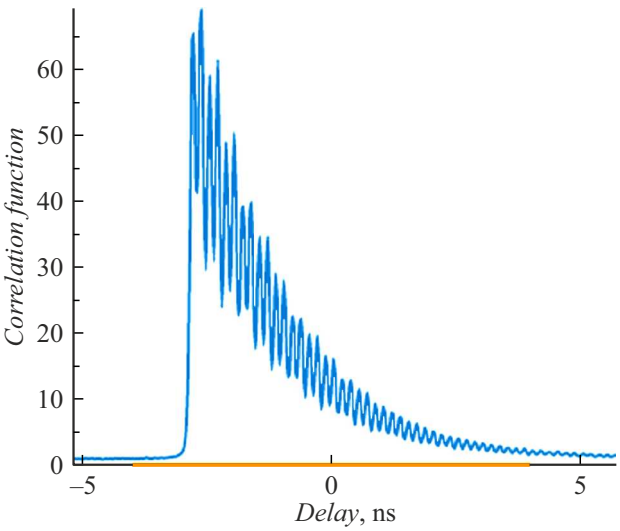

Figure 6. Typical form of a normalized correlation function during tuning of the confocal Fabry–Perot interferometer.

per hour. Therefore, the heralding channel width shall be about 600 MHz.

Filtration of the heralding channel used: the thermally-stabilized Fabry–Perot etalon with FSR of 20 GHz, peak width of 660 MHz and transmission coefficient of 60 % and the thermally-stabilized Fabry–Perot interferometer with FSR of 70 GHz, line width of 7 GHz and transmission coefficient of 85 %. Filter frequency stability within the line FWHM was $\sim$ 1 h.

For tuning, supplementary laser light was introduced into the single-photon source at the signal channel frequency and was spatially matched with the pump. Radiation was generated in the MgO:PPLN crystal at a difference frequency that inherently satisfied relation (1). Filters were set to maximum transmission.

The created source had a heralding efficiency of about 0.6 %. Pair generation rate was 100 cps with a pump power of 3.2 mW and 30 cps with a pump power of 1 mW.

Note that the difference frequency radiation may be used both for initial tuning and routine adjustment during measurements. Automatic adjustment procedure may be potentially implemented. Due to this a filtration system with a smaller width may be used and heralding efficiency may be improved.

To check spectral matching with the quantum memory signal transition, absorption of single-photon source radiation was measured. Ideally almost total absorption could be expected. Unfortunately, only one third of heralded photons was absorbed in our case. This suggests the filtration system was imperfect. However, taking into account that the spectrum width decreased approximately by a factor of 1000, such result may be treated as satisfactory.

When using the quantum memory, a single-photon source signal was sent directly to the polarizing beam splitter (Figure 1), where its was aligned with laser light. To check the quality of alignment, both signals were collimated into the same single-mode fiber. To reduce the integration time, it was reasonable to increase the ratio between the memory utilization and preparation times even by means of mean efficiency reduction. For this, the chopper operation mode was changed. The chopper *11*, which blocked the single-photon detector, was opened for a half-period. In the first half of the period (with closed detector), AFC was prepared, in the second half of the period, AFC was used. To improve the signal-to-noise ratio, detector signal strobe mode was implemented and only the events taking place during the memory running time were detected. AFC was created using a periodic sequence of laser pulses with a duration of 12 ns and period of 60 ns. The chopper *7* was opened for the comb burning time and cut out a pulse with the desired duration from the sequence. Measurements have shown that 3 ms was sufficient for this when the intensity was $\sim$ 10 mW. Thus, the preparation time could be reduced and chopper rotation frequency could be increased, which also reduced the average time between the AFC creation and its utilization.

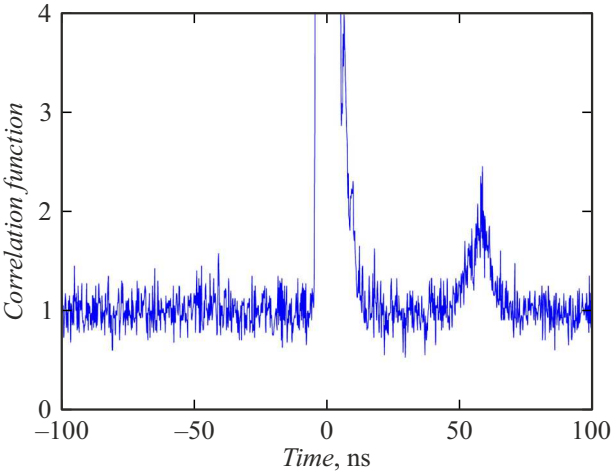

Figure 7. Echo from single-photon source radiation

Experiment for single-photon source signal storage was conducted as follows. Burning sequence of laser pulses was created using the AOM. The chopper *7* was set to 46 Hz and cut a 3 ms pulse from the sequence. After a 5 ms delay required for the residual fluorescence decay, the single-photon detector was opened, and the signal was written and detected for a half-period. The expected memory efficiency may be estimated by averaging the efficiency dependence over the observation time. Taking into account that only one third of heralded photons interacts with the AFC, the estimated value is about 1.5 %.

The experiment time was 3 h. Correlation function between the signal channel and the heralding channel was measured. The measurement results are shown in Figure 7. Echo can be seen 60 ns after the written pulse. The signal-to-noise ratio is about one. Efficiency calculated as the ratio of echo count to the total count of heralded photons was approximately equal to 1 %, which was a little less than the expected efficiency. This may be caused by insufficient spatial matching between the source and the quantum memory.

Conclusion

The work describes the results of the research towards implementing solid-state quantum memory for optical signals at the single-photon level. Isotopically pure $^{143}Nd^{3+}:Y^7LiF_4$ crystal cooled to cryogenic temperatures, having a sufficiently strong optical transition $^4I_{9/2}(1)-^4F_{3/2}(1)$ with a wavelength of $\sim$ 867 nm within the optical fiber transmission window was used as the medium. The isotopically pure crystal provided small inhomogeneous broadening of $\sim$ 100 MHz, due to which the desired working line could be located within the complex transition structure. The memory was implemented using the atomic frequency comb protocol that had a set of potential benefits: high multimode capacity, relatively

simple experimental implementation. Experiments with weakened laser pulses with a average number of photons per pulse on the order of one have demonstrated optical signal storage with times of 60 ns, efficiency of 6.4 % and a signal-to-noise ratio of ~ 3. A single-photon source spectrally matched with the quantum memory bandwidth based on spontaneous parametric down conversion in a periodically-poled MgO : PPLN crystal was created. Single-photon source signal storage was demonstrated.

Funding

The study was funded by the Ministry of Science and Higher Education of the Russian Federation within the Program of the Center of Excellence „Center of Photonics“.

Conflict of interest

The authors declare no conflict of interest.

References

[1] K. Heshami, D.G. England, P.C. Humphreys, P.J. Bustard, V.M. Acosta, J. Nunn, B.J. Sussman. J. Modern Optics, **63**, 2005 (2016). DOI: 10.1080/09500340.2016.1148212
[2] M. Zhong, M.P. Hedges, R.L. Ahlefeldt, J.G. Bartholomew, S.E. Beavan, S.M. Wittig, J.J. Longdell, M.J. Sellars. Nature, **517**, 177 (2015). DOI: 10.1038/nature14025
[3] Yi-Lin Hua, Zong-Quan Zhou, Chuan-Feng Li, Guang-Can Guo. Chin. Phys. B, **27**, 020303 (2018). DOI: 10.1088/1674-1056/27/2/020303
[4] M. Guo, S. Liu, W. Sun, M. Ren, F. Wang, M. Zhong. Front. Phys., **18**, 21303 (2023). DOI: 10.1007/s11467-022-1240-8
[5] Zhu Tian-Xiang, Liu Xiao, Zhou Zong-Quan, Li Chuan-Feng. Nanophotonics, (2025). DOI: 10.1515/nanoph-2024-0487
[6] R.M. Macfarlane. J. Lumin., **100**, 1 (2002). DOI: 10.1016/S0022-2313(02)00450-7
[7] G. Heinze, C. Hubrich, T. Halfmann. Phys. Rev. Lett., **111**, 033601 (2013). DOI: 10.1103/PhysRevLett.111.033601
[8] J.J. Longdell, E. Fraval, M.J. Sellars, N.B. Manson. Phys. Rev. Lett., **95**, 063601 (2005). DOI: 10.1103/PhysRevLett.95.063601
[9] A.L. Alexander, J.J. Longdell, M.J. Sellars N.B. Manson. Phys. Rev. Lett., **96**, 043602 (2006). DOI: 10.1103/PhysRevLett.96.043602
[10] M. Hedges, J.J. Longdell, Y. Li, M.J. Sellars. Nature, **465**, 1052 (2010). DOI: 10.1038/nature09081
[11] V. Damon, M. Bonarota, A. Louchet-Chauvet, T. Chaneliére, J.-L. Le Gouët. New J. Phys., **13**, 093031 (2011). DOI: 10.1088/1367-2630/13/9/093031
[12] K.I. Gerasimov, M.M. Minnegaliev, S.A. Moiseev, R.V. Urmancheev, T. Chanelife, A. Louchet-Chauvet. Opt. Spectr., **123**, 211 (2017). DOI: 10.1134/S0030400X17080069
[13] M. Afzelius, C. Simon, H. De Riedmatten, N. Gisin. Phys. Rev. A, **79**, 052329 (2009). DOI: 10.1103/PhysRevA.79.052329
[14] M. Bonarota, J.-L. Le Gouët, T. Chaneliére. New J. Phys., **13**, 013013 (2011). DOI: 10.1088/1367-2630/13/1/013013
[15] N. Sinclair, E. Saglamyurek, H. Mallahzadeh, J.A. Slater, M. George, R. Ricken, M.P. Hedges, D. Oblak, C. Simon, W. Sohler, W. Tittel. Phys. Rev. Lett., **113**, 053603 (2014). DOI: 10.1103/PhysRevLett.113.053603
[16] R.A. Akhmedzhanov, L.A. Gushchin, A.A. Kalachev, S.L. Korableva, D.A. Sobgayda, I.V. Zelensky. Laser Phys. Lett., **13**, 015202 (2016). DOI: 10.1088/1612-2011/13/1/015202
[17] R.A. Akhmedzhanov, L.A. Gushchin, A.A. Kalachev, N.A. Nizov, V.A. Nizov, D.A. Sobgayda, I.V. Zelensky. Laser Phys. Lett., **13**, 115203 (2016). DOI: 10.1088/1612-2011/13/11/115203
[18] R.A. Akhmedzhanov, L.A. Gushchin, I.V. Zelensky, V.A. Nizov, N.A. Nizov, D.A. Sobgaida. Radiophys. Quantum El., **67**, 121 (2024). DOI: 10.1007/s11141-025-10359-6
[19] N. Sangouard, C. Simon, H. De Riedmatten, N. Gisin. Rev. Mod. Phys., **83**, 33 (2011). DOI: 10.1103/RevModPhys.83.33
[20] M.D. Eisaman, J. Fan, A. Migdall, S.V. Polyakov. Rev. Sci. Instrum., **82**, 071101 (2011). DOI: 10.1063/1.3610677
[21] S. Tanzilli, A. Martin, F. Kaiser, M.P. De Micheli, O. Alibart, D.B. Ostrowsky. Laser Photon. Rev., **6**, 115 (2012). DOI: 10.1002/lpor.201100010
[22] I.Z. Latypov, A.V. Shkalikov, D.O. Akat'ev, A.A. Kalachev. J. Phys.: Conf. Ser., **859**, 012011 (2017). DOI: 10.1088/1742-6596/859/1/012011
[23] I. Usmani, C. Clausen, F. Bussiéres, N. Sangouard, M. Afzelius, N. Gisin. Nature Photon., **6**, 234 (2012). DOI: 10.1038/NPHOTON.2012.34
[24] A.L. Harmer, A. Linz, D.R. Gabbe. J. Phys. Chem. Solids, **30**, 1483 (1969). DOI: 10.1016/0022-3697(69)90210-8

Translated by E.Ilinskaya